the plant journal

SEB Society for Experimental Biology

The Plant Journal (2015) **81,** 147–159 doi: 10.1111/tpj.12682

TECHNICAL ADVANCE

A fluorescence-activated cell sorting-based strategy for rapid isolation of high-lipid *Chlamydomonas* mutants

Mia Terashima[1], Elizabeth S. Freeman[1,2], Robert E. Jinkerson[1] and Martin C. Jonikas[1,*]

[1]*Department of Plant Biology, Carnegie Institution for Science, 260 Panama Street, Stanford, CA 94305, USA, and*

[2]*Department of Biology, Stanford University, Stanford, CA 94305, USA*

Received 11 December 2013; revised 22 August 2014; accepted 19 September 2014; published online 29 September 2014.

*For correspondence (e-mail mjonikas@carnegiescience.edu).

SUMMARY

There is significant interest in farming algae for the direct production of biofuels and valuable lipids. *Chlamydomonas reinhardtii* is the leading model system for studying lipid metabolism in green algae, but current methods for isolating mutants of this organism with a perturbed lipid content are slow and tedious. Here, we present the *Chlamydomonas* high-lipid sorting (CHiLiS) strategy, which enables enrichment of high-lipid mutants by fluorescence-activated cell sorting (FACS) of pooled mutants stained with the lipid-sensitive dye Nile Red. This method only takes 5 weeks from mutagenesis to mutant isolation. We developed a staining protocol that allows quantification of lipid content while preserving cell viability. We improved separation of high-lipid mutants from the wild type by using each cell's chlorophyll fluorescence as an internal control. We initially demonstrated 20-fold enrichment of the known high-lipid mutant *sta1* from a mixture of *sta1* and wild-type cells. We then applied CHiLiS to sort thousands of high-lipid cells from a pool of about 60 000 mutants. Flow cytometry analysis of 24 individual mutants isolated by this approach revealed that about 50% showed a reproducible high-lipid phenotype. We further characterized nine of the mutants with the highest lipid content by flame ionization detection and mass spectrometry lipidomics. All mutants analyzed had a higher triacylglycerol content and perturbed whole-cell fatty acid composition. One arbitrarily chosen mutant was evaluated by microscopy, revealing larger lipid droplets than the wild type. The unprecedented throughput of CHiLiS opens the door to a systems-level understanding of green algal lipid biology by enabling genome-saturating isolation of mutants in key genes.

Keywords: *Chlamydomonas reinhardtii*, triacylglycerol, high-throughput, fluorescence-activated cell sorting, mutant screen, Nile Red, lipids, technical advance.

INTRODUCTION

Green algae are a promising platform for photosynthetic and heterotrophic production of high-value lipids and biofuels. Some species are capable of very high growth rates (one to three population doublings per day) in saline or brackish water, for which there is little agricultural demand. Many species have been found to accumulate large amounts of lipids (20–80% of dry weight) as triacylglycerols (TAGs), which can be converted to biofuels (Chisti, 2008; Hu *et al.*, 2008; Grobbelaar, 2010; Stephenson *et al.*, 2011; Liu *et al.*, 2012). The accumulation of TAG is often induced under stressful growth conditions (Tonon *et al.*, 2002; Wijffels and Barbosa, 2010), such as nitrogen deprivation (Wang *et al.*, 2009; Moellering and Benning, 2010). These considerations, combined with projections from laboratory data, have led to estimates that algae could be engineered to produce an amount of biofuel per land area comparable to the potential of cellulosic crops (Dismukes *et al.*, 2008).

Despite the ongoing interest in algal lipid production, our understanding of algal lipid metabolism is in its infancy. In green algae, several classes of lipids seem to be absent, and pathway organization and regulation are only beginning to be understood (Giroud *et al.*, 1988; Riekhof *et al.*, 2005; Chang *et al.*, 2011; Liu and Benning, 2012). More broadly, key elements of lipid metabolism in photosynthetic eukaryotes remain unknown, such as the pathway of export of fatty acids from the site of synthesis in the chloroplast stroma to the endoplasmic reticulum.

The green alga *Chlamydomonas reinhardtii* has a unique combination of features that make it a particularly powerful model system for studying lipid metabolism in green algae, with the potential to guide metabolic engineering efforts in production organisms (Merchant *et al.*, 2012). Its nuclear, chloroplast and mitochondrial genomes are all sequenced and transformable. It grows as a haploid, allowing immediate observation of the phenotypes of recessive mutations. It has a well-characterized sexual cycle, enabling rapid combination of mutations through genetic crosses. It grows rapidly, with a doubling time of 6–10 h. Finally, it benefits from a powerful molecular toolkit, including insertional mutagenesis and inducible expression vectors (Harris *et al.*, 2009). Despite these attractive features, only a handful of *C. reinhardtii* mutants with perturbed lipid accumulation have been isolated.

Mutants perturbed in starch synthesis, cell cycle control and TAG synthesis have been found to affect TAG accumulation (Posewitz *et al.*, 2004; Wang *et al.*, 2009; Li *et al.*, 2010a; Work *et al.*, 2010; Goodson *et al.*, 2011; Siaut *et al.*, 2011; Yao *et al.*, 2012; Velmurugan *et al.*, 2013). A block in starch synthesis in *sta1*, *sta6* and *sta7-10* mutants leads to a diversion of carbon to lipids, resulting in increased TAG accumulation (Ball *et al.*, 1991; Zabawinski *et al.*, 2001; Posewitz *et al.*, 2004; Wang *et al.*, 2009; Li *et al.*, 2010a,b; Work *et al.*, 2010; Goodson *et al.*, 2011; Siaut *et al.*, 2011; Velmurugan *et al.*, 2013). A mutant in a galactolipid lipase, PGD1, thought to be required for export of fatty acids from the chloroplast, showed reduced TAG accumulation (Li *et al.*, 2012b). Mutants in phospholipid:diacylglycerol acyltransferase (PDAT), which produces TAG by transferring an acyl group from a phospholipid to diacylglycerol, also have reduced TAG accumulation (Boyle *et al.*, 2012; Yoon *et al.*, 2012). Finally, a knock-down of the lipase LIP1 resulted in delayed TAG turnover after nitrogen replenishment (Li *et al.*, 2012a).

The complexity of lipid pathways and the number of candidate genes involved in the process suggest that mutant screens to date have not approached saturation. Bioinformatics analyses of the *Chlamydomonas* genome sequence predicted a core set of pathways in lipid metabolism by analogy with known organisms (Riekhof *et al.*, 2005; Chang *et al.*, 2011). Mutants in most of the predicted enzymes have not been isolated or analyzed.

The labor-intensive nature of existing screening methods prohibits saturating identification of genes with roles in lipid accumulation. The largest screen so far of lipid content in *Chlamydomonas* mutants used a plate reader to screen 34 000 mutants and identified 80 putative mutants with perturbed lipid content, of which six were reproducible (Li *et al.*, 2012b). Yan *et al.* (2013) analyzed 7000 mutants in a similar manner and identified 10 putative mutants with decreased oil accumulation.

Flow cytometry allows analysis of the lipid content on a single-cell basis (Hyka *et al.*, 2013). Lipid-binding dyes including Nile Red and BODIPY are used to quantify the lipid content in individual cells (Greenspan *et al.*, 1985; Moellering and Benning, 2010; Cirulis *et al.*, 2012). One study found that Nile Red is preferable to BODIPY for staining of microalgae, because the Nile Red fluorescence signal is less sensitive to the overall dye concentration (Cirulis *et al.*, 2012). A recent study by Cagnon *et al.* (2013) used flow cytometry to identify mutants with perturbed lipid content from a collection of 1800 transformants, and successfully confirmed phenotypes in 31 mutants, but the throughput of the approach (96 strains per hour) prohibits screening of collections large enough to approach genome saturation.

Fluorescence-activated cell sorting (FACS) allows isolation of cells that show desirable characteristics by flow cytometry. FACS has been used to enrich for high-lipid strains of *Tetraselmis suecica* (Montero *et al.*, 2011) and to isolate high-lipid mutants of *Nannochloropsis* (Doan and Obbard, 2011a, 2012) and *Chlorella* (Manandhar-Shrestha and Hildebrand, 2013). Recently, two studies used FACS to measure and recover BODIPY- and Nile Red-stained *Chlamydomonas* mutant cells (Velmurugan *et al.*, 2013; Xie *et al.*, 2014), but enrichment of strains with high lipid content by FACS was not demonstrated. In this work, we present *Chlamydomonas* high-lipid sorting (CHiLiS), a one-step FACS enrichment strategy enabling efficient screening of tens of thousands of *C. reinhardtii* mutants for high lipid content.

RESULTS

CHiLiS is a rapid method for isolating large numbers of *C. reinhardtii* mutant strains with increased lipid accumulation

CHiLiS takes a total of 5 weeks from mutagenesis to the generation of an arrayed library. Using Nile Red staining to quantify neutral lipid content, high-lipid mutants are isolated by FACS. The process starts with (i) insertional mutagenesis, followed by (ii) 2 weeks of recovery on plates, (iii) mutant pooling into a single culture and growth for 3 days, (iv) nitrogen deprivation for 3 days to induce lipid accumulation, (v) Nile Red staining and FACS sorting of high-lipid cells, (vi) recovery of mutant colonies on plates for 2 weeks, and (vii) confirmation of the phenotypes of isolated mutants (Figure 1).

Nile Red and chlorophyll fluorescence of *Chlamydomonas* cells can be fully resolved by flow cytometry

We measured Nile Red by excitation with a 488-nm laser and capturing the emission with a 525/50 bandpass filter. Chlorophyll fluorescence was measured by exciting at 633 nm and capturing emission with a 670/30 bandpass

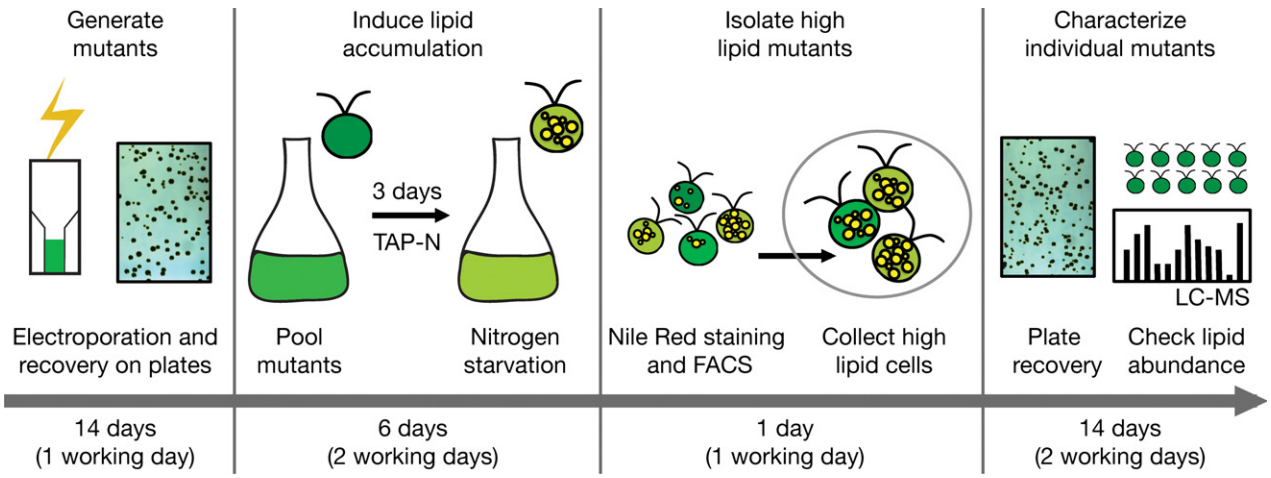

Figure 1. Schematic of the screen developed in this work. We have developed a screen that takes 5 weeks from mutagenesis to a collection of colonies enriched in high-lipid mutants. TAP-N, 2-amino-2-(hydroxymethyl)1,3-propanediol (TRIS)-acetate-phosphate with low nitrogen; FACS, fluorescence-activated cell sorting; LC-MS, liquid chromatography–mass spectrometry.

filter (Figure 2). Point-scanning confocal analysis confirmed that the Nile Red signal captured by the 525/50 filter originates from structures resembling lipid droplets, and signals from other fluorescent features (e.g. chlorophyll in chloroplasts) are excluded by this filter (Figure 2c). In the Nile Red channel, Nile Red-stained cells were about 50 times brighter than the signal from autofluorescence (Figures 2e and S1). We conclude that for Nile Red-stained cells, the Nile Red stain produces about 98% of the signal measured in the Nile Red channel, and the contribution of other sources of fluorescence (including chlorophyll fluorescence) to this signal is negligible.

Point-scanning confocal analysis confirmed that the chlorophyll signal captured by the 670/30 filter originates from the chloroplast, and signal from Nile Red-stained lipid bodies is excluded by this filter (Figure 2d). The chlorophyll signal is not significantly perturbed by Nile Red staining (Figure 2f). We conclude that there is no measurable bleed-through from the Nile Red stain into the chlorophyll channel.

The addition of detergent improves the uniformity of Nile Red staining

In our initial experiments, we encountered difficulties in attempts to stain all cells uniformly with Nile Red. We observed bimodal staining when we stained cells that had been deprived of nitrogen for 3 days (Figures 3 and S2). Instead of a gradient of fluorescence intensities, it appeared that a subpopulation of cells showed fluorescence emission levels similar to those of unstained cells. Poor staining of cell populations with Nile Red has been a challenge in other algal species, and has been improved in other algae by modifications to the staining procedure, such as the addition of glycerol (Doan and Obbard, 2011b) or by microwaving the cells (Chen *et al.*, 2011).

We found that the addition of low levels of the detergent Triton X-100 increased the homogeneity of staining of *Chlamydomonas* cells, suggesting that the bimodal staining property was probably due to decreased penetration of dye in a fraction of the cells, rather than a bimodal distribution of lipid accumulation. By adding a titration of 0.004–0.012% Triton X-100 during staining, we found a dose-dependent decrease in the fraction of unstained cells (Figure 3). At or above 0.014% Triton X-100, we found that the cells had lower staining uniformity. Microscopic analysis of cells treated with 0.014% Triton X-100 revealed an unusual morphology, suggesting that at or above this concentration Triton X-100 perturbs cellular organization (Figure S3). We consistently saw maximal homogeneity of staining at 0.010–0.012% Triton X-100. For subsequent experiments, we used 0.011% Triton X-100 to improve the homogeneity of Nile Red staining.

Nile Red staining and chlorophyll fluorescence are correlated at the single-cell level

We observed a strong correlation between the Nile Red and chlorophyll channel intensities of each cell (Figure 3). Others have also found similar correlations in the intensities of these channels in *Chlamydomonas* (Cagnon *et al.*, 2013). The data shown in Figure 2 indicate that bleed-through between the channels in stained cells is around 2%, eliminating the possibility that this correlation is an artifact of bleed-through from one channel to the other. Instead, our data indicate that there is a strong correlation between the intensity of Nile Red staining and chlorophyll fluorescence at a single-cell level. This is probably due to a biological correlation between lipid accumulation and

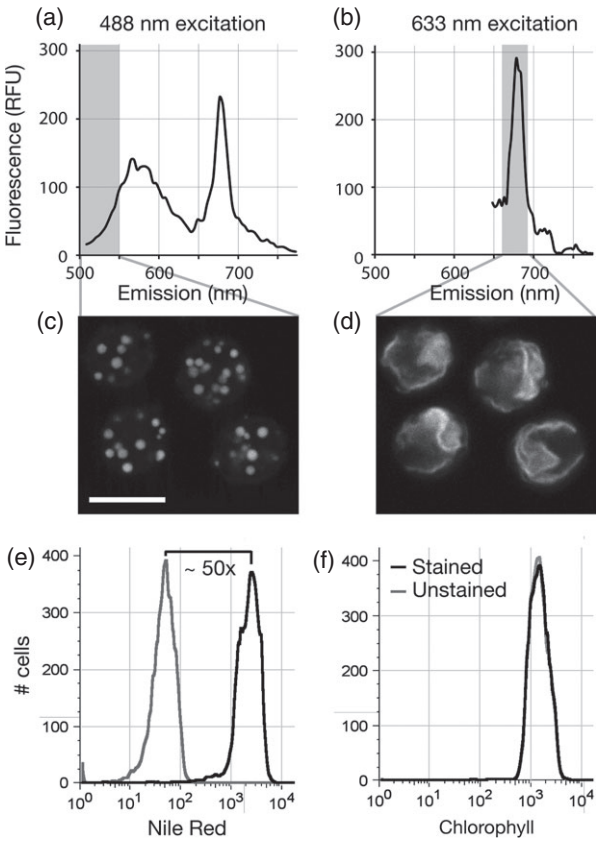

Figure 2. The emission spectra of chlorophyll and Nile Red can be resolved. Cells that were nitrogen-starved for 3 days were stained with Nile Red and the emission spectra at excitation wavelengths of 488 and 633 nm were analyzed using a point-scanning confocal microscope.
(a) Emission scan of an entire cell at 488 nm excitation. RFU, relative fluorescence units.
(b) Emission scan of an entire cell at 633 nm excitation. In (a) and (b) the wavelength ranges used to capture the Nile Red and chlorophyll fluorescence in flow cytometry are highlighted in gray.
(c) Cells were illuminated at 488 nm and an image was generated from emitted light in the range of 500–550 nm. Bar: 10 μm.
(d) Cells were illuminated at 633 nm and an image was generated from emitted light in the range of 655–685 nm.
(e) Flow cytometry was used to collect signal intensity in the Nile Red channel from stained and unstained cells.
(f) Flow cytometry was used to collect signal intensity in the chlorophyll channel from stained and unstained cells.

chlorophyll content on a single-cell basis; for example, larger cells could contain more of both.

Comparison of Nile Red with chlorophyll fluorescence improves our ability to resolve differences in single-cell lipid content

The ability to efficiently enrich mutants with modest increases in lipid content is made challenging by the fact that there is significant overlap between the Nile Red distributions of the desired mutants and the wild type (Figure S4a). This overlap is due to two factors: (i) the difference in average lipid content between the mutant and

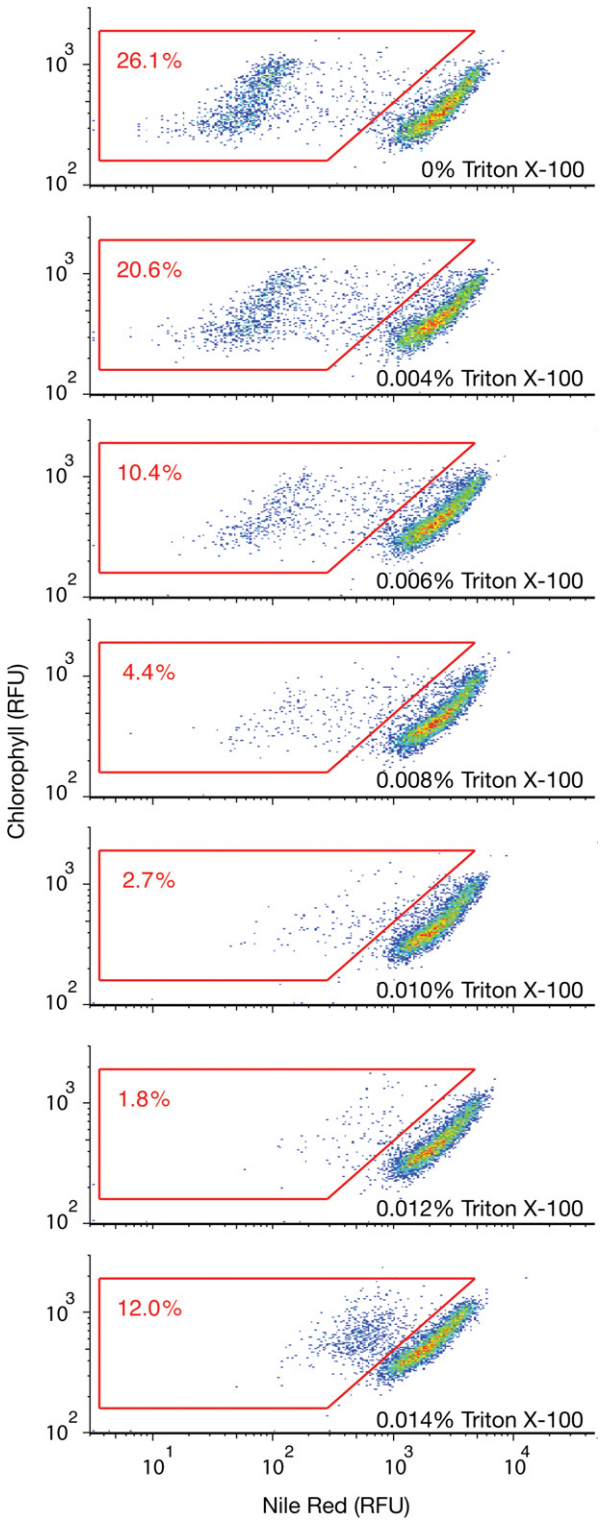

Figure 3. Detergent increases staining homogeneity. Nile Red staining without detergent results in a bimodal staining distribution in the Nile Red channel. A gate was drawn that includes most cells with Nile Red fluorescence lower than the high Nile Red population. The percentage of all cells that fell into this gate are indicated in the gate. The same experiment was performed with the indicated increasing amounts of Triton X-100. Each plot represents 10 000 cells. RFU, relative fluorescence units.

wild-type strains is relatively small (e.g. *sta1* and wild-type lipid content differ by approximately twofold) and (ii) the variation in lipid content of individual cells from a single genotype is relatively large (around tenfold) (Figure 4a–c).

Before attempting to screen for new mutants, we sought to optimize our ability to distinguish between the high-lipid-accumulating starchless strain *sta1* (also known as I7) (Ball *et al.*, 1991; Siaut *et al.*, 2011) and its background wild-type strain 137c by considering other parameters measured in individual cells. We presumed that much of the variation in the lipid content of individual cells from a single genotype was due to extrinsic noise factors such as cell size or metabolic state (Elowitz *et al.*, 2002). We sought a measurable parameter that would report on these extrinsic noise factors but was independent of lipid accumulation. Forward scatter, which is often used as a readout of cell size, was considered but could not cleanly resolve *sta1* from wild-type populations (Figure S4b).

Chlorophyll fluorescence is a prime candidate for a parameter for reporting on extrinsic noise factors that affect lipid content. Our observation of a strong correlation between single-cell chlorophyll fluorescence and Nile Red staining within isogenic populations (Figures 3 and 4), with the two channels being nearly free of bleed-through (Figure 2), suggested that chlorophyll fluorescence is affected by many of the same extrinsic noise factors that affect lipid content. As the chlorophyll biosynthesis pathway is independent of the TAG synthesis pathway, mutations that specifically perturb lipid content are not expected to directly perturb chlorophyll content. In addition, chlorophyll fluorescence has been successfully used as an internal standard in microplate assays with Nile Red (Li *et al.*, 2012b). When plotted in the two dimensions of chlorophyll and Nile Red fluorescence, the *sta1* and wild-type populations were nearly fully resolved (Figure 4a–c), indicating that comparison of Nile Red with chlorophyll fluorescence improves the resolution of differences in *Chlamydomonas* lipid content beyond what is achievable with forward scatter and Nile Red (Figure S4b) or Nile Red alone (Figure S4a).

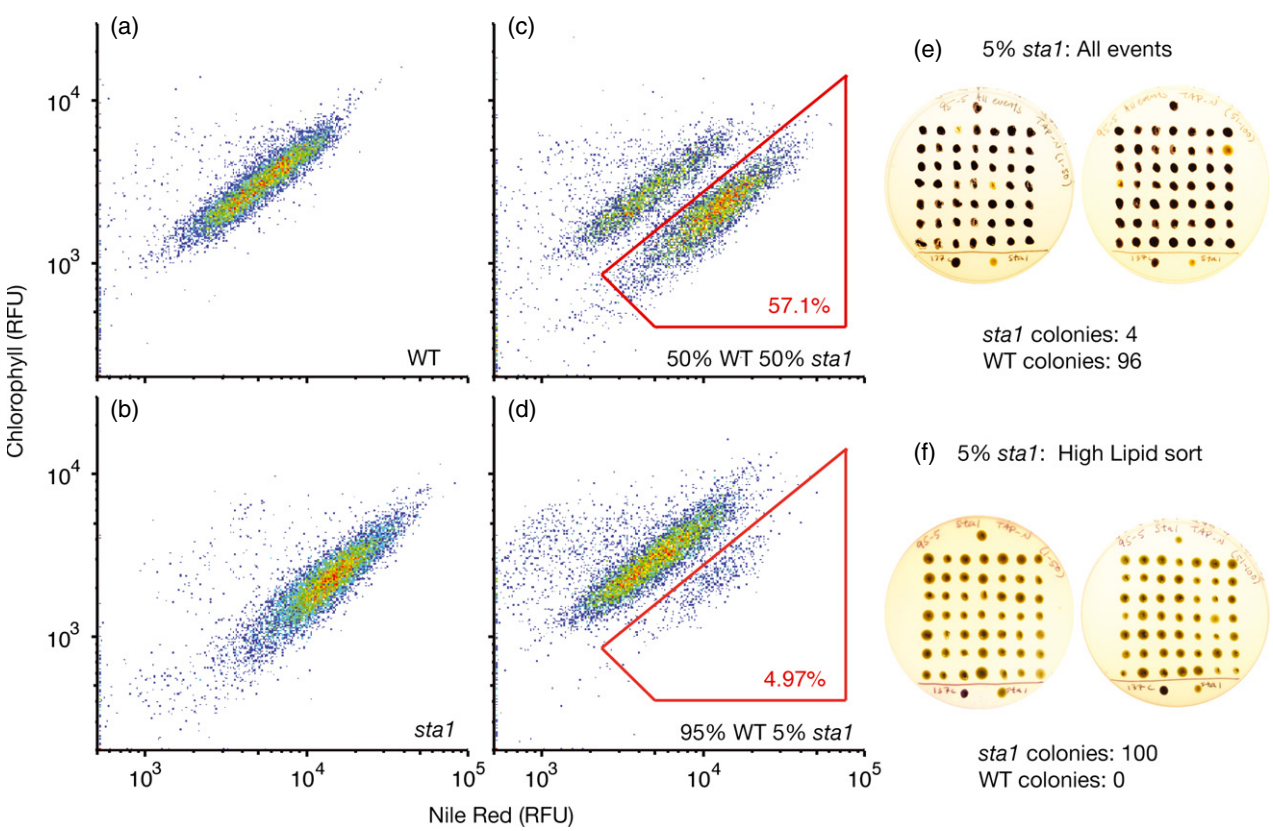

Figure 4. We are able to precisely isolate *sta1* mutants from the wild type by FACS.
(a–d) Flow cytometry analysis of Nile Red-stained wild-type 137c (WT) and the *sta1* mutant. Each plot represents 10 000 cells. In (c), when similar amounts of the wild-type 137c strain and *sta1* strain are mixed, two distinct populations can be observed. A high-lipid gate was drawn to encompass only the *sta1* population. The number in the gate represents the percentage of all measured cells that fall into the gate. RFU, relative fluorescence units. (d) We mixed 5% *sta1* and 95% wild-type cells and sorted out either all measured cells or only the cells that fell into the *sta1* gate.
(e–f) Patches of cells from colonies picked at random from (e) 'all events' or sorted (f) 'high-lipid' cells were stained with iodine vapors to test for the starchless phenotype. The patches below the horizontal lines are the 137c wild type and *sta1* controls.

We therefore used a two-dimensional sorting gate defined by Nile Red and chlorophyll, which allows comparison of the Nile Red fluorescence of each cell with that of other cells of similar chlorophyll content (Figure 4c). In addition to the improved resolution of high-lipid mutants, one benefit of this approach is that larger or clumped cells are less likely to be falsely identified as high-lipid cells, because their combined higher Nile Red fluorescence is accompanied by higher chlorophyll fluorescence. One potential drawback of this approach is that it would also be expected to enrich for low-chlorophyll mutants; however, such mutants can easily be removed in a secondary screen.

The known high-lipid *sta1* mutant can be efficiently enriched by FACS

We tested our ability to enrich for high-lipid mutant cells from a background of wild-type cells using FACS (Figure 4d–f). We were able to effectively isolate *sta1* from a mixture of 5% *sta1* and 95% wild-type cells (Figure 4e). Iodine staining of 100 colonies picked from plates containing recovered cells showed that all 100 isolated colonies exhibited a starchless phenotype (a 20-fold enrichment) (Figure 4f).

A pool of approximately 60 000 mutants shows a wider Nile Red fluorescence distribution than the wild type

We generated approximately 60 000 mutants through random insertional mutagenesis by electroporating a cassette conferring resistance to paromomycin into cells of the wild-type CMJ030 strain (Chlamydomonas Resource Center CC-4533, http://chlamycollection.org/) (Zhang *et al.*, 2014). We selected for mutants on 2-amino-2-(hydroxymethyl)1,3-propanediol (TRIS)-acetate-phosphate (TAP) plates containing paromomycin. After 2 weeks of growth on plates, we pooled all colonies into a single liquid culture by scraping cells from the plates. We grew the culture for 3 days in TAP, and then transferred the cells to TAP-N (low nitrogen) for 3 days to induce lipid accumulation.

We stained nitrogen-deprived cells with Nile Red and compared the fluorescence distribution of the mutant pool with the distribution of the wild-type CMJ030 strain (Figure 5). The mutant pool showed a wider Nile Red fluorescence distribution than did CMJ030. We drew a 'high-lipid' gate that captured about 1% of the wild-type CMJ030 cells with maximal Nile Red fluorescence signal for a given chlorophyll fluorescence signal (Figure 5a). The same gate captured about 6% of the cells in the mutant pool (Figure 5b). A wider Nile Red and chlorophyll signal distribution in the pool of mutants indicates the presence of mutants that accumulate higher and lower amounts of lipid and chlorophyll.

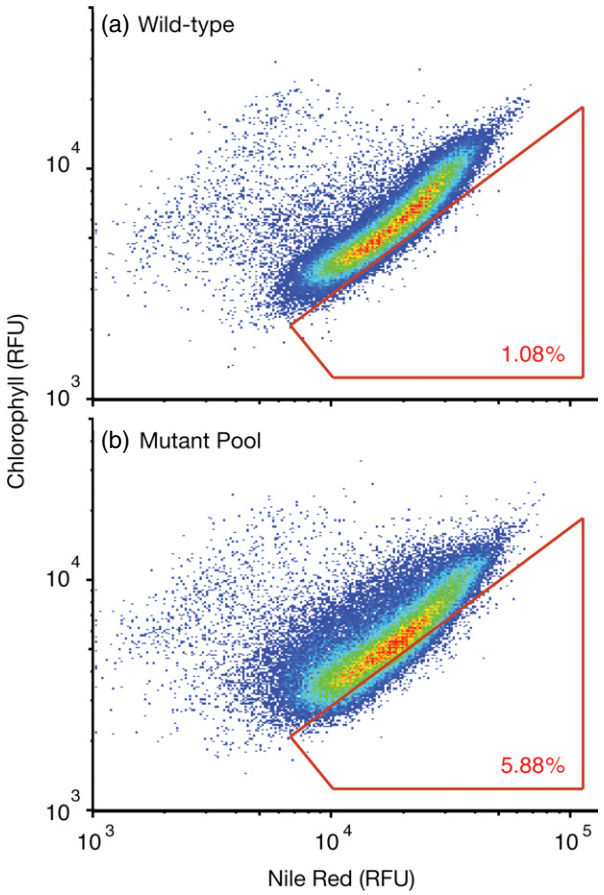

Figure 5. Our mutagenized population contains more high-lipid cells than a wild-type population.
(a) A high-lipid gate was drawn on a wild-type population to encompass 1% of cells with maximal Nile Red fluorescence signal for a given chlorophyll fluorescence signal. RFU, relative fluorescence units.
(b) A pool of approximately 60 000 mutants has approximately 6% cells in the same high-lipid gate. Each plot represents 100 000 cells.

We used FACS to enrich a pool of 60 000 mutants for high-lipid mutants

We analyzed 320 million cells and sorted 19 million cells that fell in the high-lipid gate. Five million isolated cells were plated on TAP agar. After 2 weeks, about 250 000 colonies were visible (approximately 5% of the plated cells gave rise to a colony). The recovery rate of the mutant pool was similar to the recovery rate of wild-type cells subjected to Nile Red staining and FACS (Figure S5).

About 50% of isolated mutants show a reproducible high-lipid phenotype by flow cytometry

We picked 28 mutant colonies from the plates for further analysis. Of the 28 mutants, four were not analyzed further because they formed extensive clumps and palmelloid colonies, which rendered flow cytometry difficult. The remaining 24 mutants were individually analyzed by flow

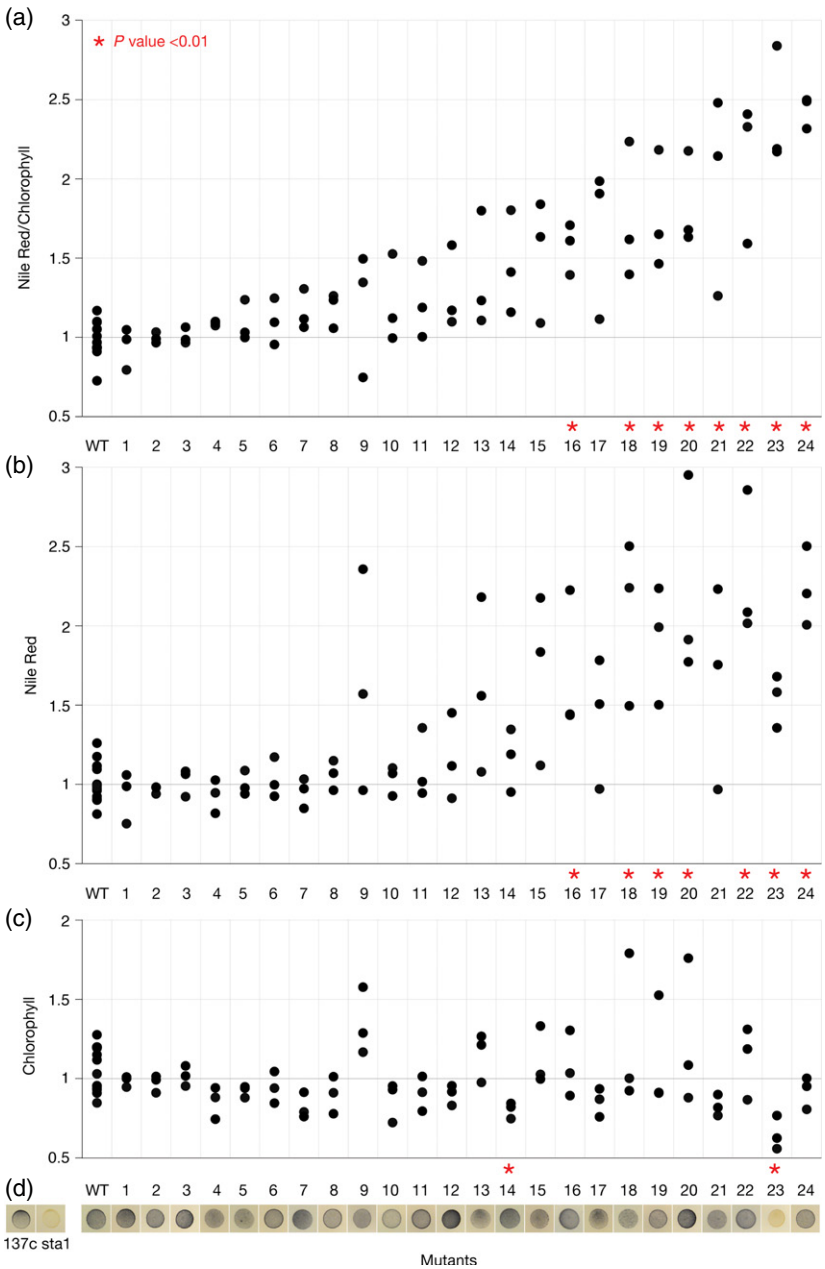

Figure 6. Isolated mutants are enriched for the high-lipid phenotype, and many of them are not starchless. Twenty-four mutants recovered from the screen were chosen at random for measurement by flow cytometry. Measurements were made in at least three biological replicates performed on different days. In each replicate, the median Nile Red and median chlorophyll fluorescence of each sample were recorded and normalized to the fluorescence of a wild-type sample. Thirteen biological replicates of an additional wild type were also measured and treated as a mutant for the purposes of statistical analyses. The mutants were arranged and numbered from lowest to highest replicate mean of the Nile Red/chlorophyll ratio. Each dot represents one replicate.
(a) The Nile Red/chlorophyll ratio.
(b) The Nile Red fluorescence.
(c) The chlorophyll fluorescence.
(d) Iodine vapors were used to stain starch in a patch of each mutant spotted on agar. **P* value < 0.01. *P*-values were calculated using the Kruskal–Wallis test.

cytometry, and the median Nile Red and chlorophyll fluorescence of each mutant was compared with that of CMJ030 (Figure 6; Table S1). Over 50% of the isolated mutants showed a reproducible increase in Nile Red/chlorophyll signal (Figure 6a); in about 30% of all mutants this increase had a statistical significance of $P < 0.01$ (Kruskal–Wallis test). Similarly, more than 50% of the isolated mutants showed a reproducible increase in Nile Red signal alone (Figure 6b). In about 30% of all mutants this increase had a statistical significance of $P < 0.01$ (Kruskal–Wallis test), and of these mutants, two had a significantly altered chlorophyll content (Figure 6c).

The lipid content and profiles of the top isolated mutants are altered

We evaluated the TAG content of nine of the top 10 isolated mutants by liquid chromatography–mass spectrometry (mutant 21 was not evaluated owing to technical problems) (Figure 7; Table S2). We found that total TAG content was increased in all nine mutants (Figure 7a). The TAG profiles of the mutants fell into three broad classes (Figure 7b): mutant 17 showed slightly increased 48:0, 50:0, and 54-carbon TAG species; mutant 23 showed increased 48- and 50-carbon TAG species and decreased

52- and 54-carbon TAG species; and the remaining mutants showed a pronounced increase in 52- and 54-carbon TAG species and a decrease in 48- and 50-carbon TAG species.

We further quantified the abundance of fatty acid classes in the same nine mutants by gas chromatography–flame ionization detection (Figure S6; Table S3). These data revealed that total fatty acid content per cell was increased in all nine mutants (Figure S6a). The fatty acid profiles also fell into three broad classes (Figure S6b): mutant 17 showed slightly increased polyunsaturated fatty acids (C18:3 and C18:4) and decreases in C16:1(3) and C16:2 (7,10); mutant 23 had slight decreases in most C18 fatty acids except for C18:1(9); and the remaining mutants showed pronounced increases in both C18:1 species and 16:1(3) with decreases in C16:0, C16:1(7), C16:1(9), C16:2, C16:4 and polyunsaturated C18 fatty acids.

The increased TAG and fatty acid abundance, as well as the perturbed lipid profiles strongly indicate that our enrichment procedure yielded bona fide high-lipid mutants with perturbed lipid metabolism.

We confirmed the high-lipid phenotype in mutant 19 by microscopy

Mutant 19 was chosen arbitrarily for further analysis by microscopy. Microscopy of BODIPY-stained cells revealed larger lipid droplets and confirmed the lower chlorophyll content in mutant 19 compared with CMJ030 (Figure 8a–f).

The top 10 isolated mutants are composed of at least six distinct strains

To determine the number of distinct strains represented in the top 10 isolated mutants, we performed Southern blots against the transformation cassette (Figure S7). We detected one insertion in each mutant.

Mutants 18, 19, 21, 22 and 24 yielded bands of a similar size, suggesting that they may be siblings of the same strain. Consistent with this possibility, the lipid profiles of mutants 18, 19, 22 and 24 are similar (Figures 7b and S6b; the lipid profile of mutant 21 was not measured). The total abundance of lipids in mutant 24 was reproducibly higher than those in the other mutants. This observation could indicate that it is a different strain; alternatively, it could be a sibling to the others that underwent epigenetic or genetic changes in the two or so years of propagation on agar between its isolation and lipidomic analyses.

Two factors could contribute to the high-frequency recovery of one strain: (i) the high lipid content of this mutant could increase its frequency of recovery over that of others, and (ii) this strain may have been more abundant than the others in the pool of mutants that was sorted, possibly due to a growth advantage. One strategy for alleviating the former problem in future screens would be to divide the mutants to be screened into multiple sorts, so that any high-lipid mutant could only dominate one sort. One strategy for alleviating the latter problem in future screens would be to pool mutants from arrayed colonies on plates; this would ensure similar numbers of starting cells across all strains.

Mutants 15, 16, 17, 20 and 23 each showed distinct Southern blot band sizes, from each other and from the remaining mutants, suggesting that the top 10 isolates are composed of at least six distinct strains. Mutants 15, 16 and 20 showed similar TAG and fatty acid profiles to mutants 18, 19, 22 and 24, although the Southern blot indicates that these mutants represent at least four distinct strains. It is possible that these strains are all mutated in the same gene(s) and/or pathways, which could result in a similar phenotype.

Only one of the high-lipid mutants is starchless

We stained the 28 mutants with iodine and found that only one mutant has a starchless phenotype (Figures 6d and S8). This indicates that many of the mutants are able to accumulate higher amounts of lipids while maintaining starch synthesis. We note that the iodine staining is not quantitative, so some mutants may have decreased starch synthesis.

DISCUSSION

High-lipid mutants isolated from our screen were able to synthesize starch

To date, many high-lipid mutants reported in *Chlamydomonas* have been associated with defects in starch biosynthesis (Ball *et al.*, 1991; Zabawinski *et al.*, 2001; Posewitz *et al.*, 2004; Wang *et al.*, 2009; Li *et al.*, 2010a,b; Work *et al.*, 2010; Goodson *et al.*, 2011; Siaut *et al.*, 2011; Velmurugan *et al.*, 2013). In contrast, nearly all of the mutants that we isolated synthesize starch. This finding raises the intriguing possibility that carbon partitioning between starch and lipids may not be the limiting factor in TAG accumulation, and that blocking starch synthesis is not necessary for high levels of TAG accumulation to be achieved. It is already known that alterations in lipid trafficking can have an effect on TAG production (Li *et al.*, 2012b), so we may expect to find more genes involved in this process in addition to genes involved in regulating lipid biosynthesis or involved in beta-oxidation.

CHiLiS increases the throughput of *Chlamydomonas* high-lipid mutant isolation

Previous high-lipid mutant screens in *C. reinhardtii* have analyzed one mutant at a time on a plate reader, by flow cytometry or by Nile Red staining of arrayed mutant colonies (Li *et al.*, 2012b; Cagnon *et al.*, 2013; Yan *et al.*, 2013; Xie *et al.*, 2014). CHiLiS is less labor-intensive and time-consuming because the initial mutants do not need to be picked and maintained. Because FACS screens about

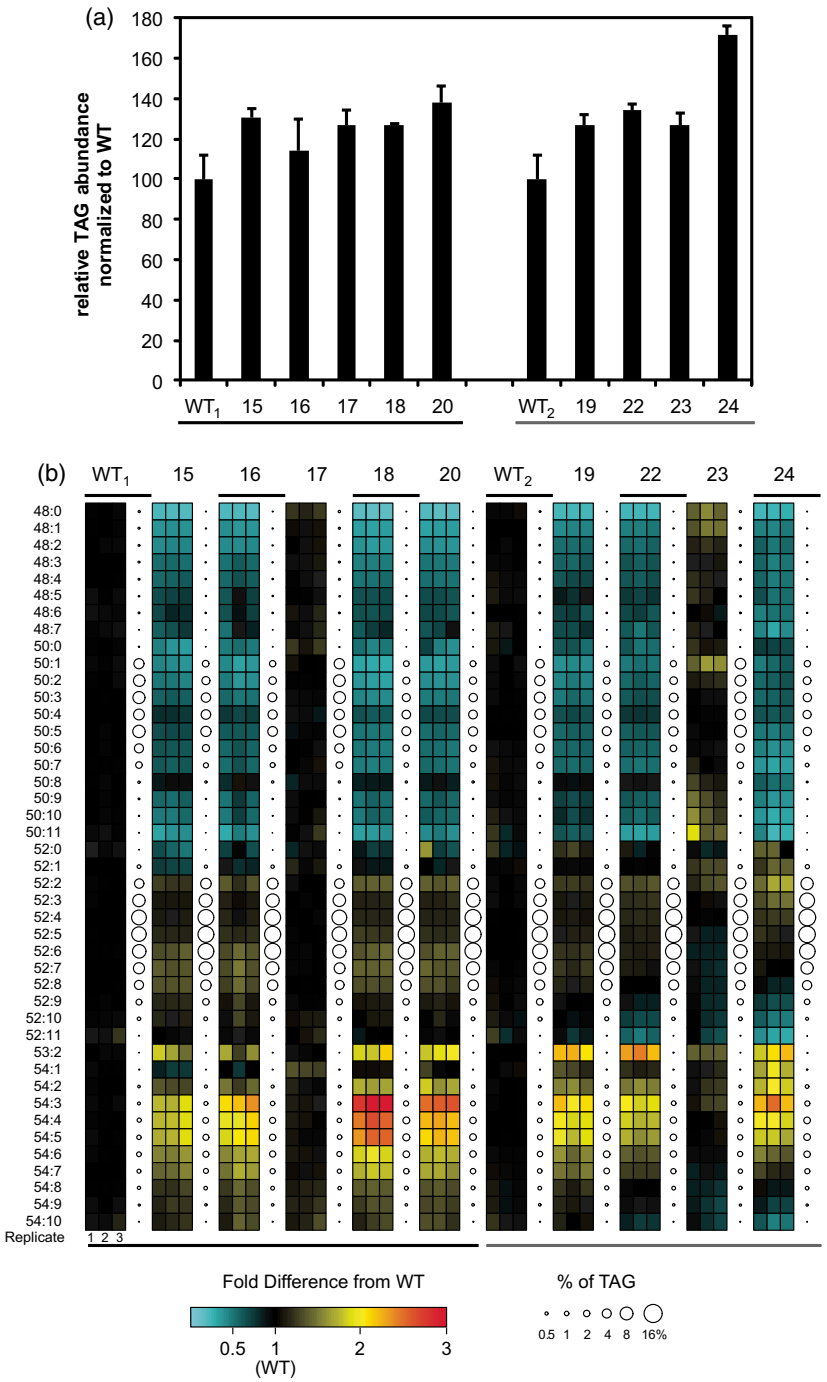

Figure 7. Lipidomics indicate increased triacylglycerol (TAG) abundance and altered TAG content in isolated mutants.

(a) Relative TAG abundance of the wild type (WT) and mutants was determined by liquid chromatography–mass spectrometry after 72 h of growth in 2-amino-2-(hydroxymethyl)1,3-propanediol (TRIS)-acetate-phosphate with low nitrogen (TAP-N). Ion counts were normalized to an internal standard (triheptadecanoin) and are displayed relative to average WT levels in each experiment. Data from two separate experiments are shown underlined by black and grey lines, with different mutants but the same wild type (WT_1 and WT_2). Bars indicate the mean of three biological replicates and error bars indicate the standard error of the mean.

(b) The relative abundance of each TAG species in each mutant is shown as a fold difference in percentage composition relative to the wild type average (colored boxes) and as a percentage of total TAG (circles). The fold difference panels represent one replicate each. The size of each circle is proportional to the percentage of total TAG represented by the corresponding TAG species, averaged over three biological replicates.

10 000 cells sec^{-1}, a substantially larger number of mutants can be quickly screened for primary hits and the phenotypes can be confirmed with more labor-intensive approaches. One added benefit of screening the mutants in a pool is a significant reduction of noise from differences in the growth environment of each mutant.

We were able to recover Nile Red-stained mutants after FACS, unlike a previous study (Velmurugan *et al.*, 2013). The difference in recovery rate may be due to the fact that we resuspended the cells in PBS after staining to remove excess Nile Red and detergent from the sample. It does appear that the staining and FACS sorting procedure reduces cell viability, as about 25% of unstained, unsorted cells gave rise to a colony, whereas only around 5% of stained and sorted cells did (Figure S5). It is possible that the plating efficiency could be improved, for example by

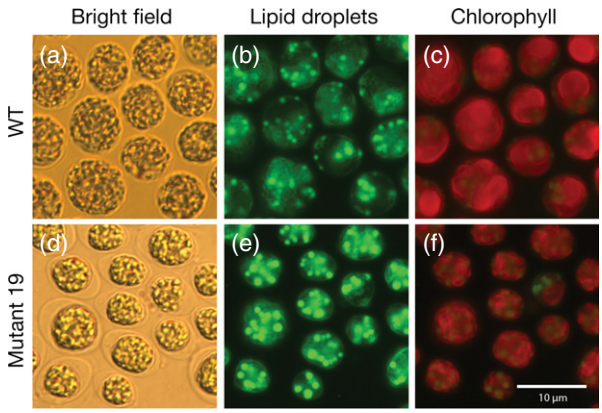

Figure 8. Mutant 19 shows larger lipid droplets than the CMJ030 wild-type.
(a–c) CMJ030 cells: (a) bright field, (b) lipids visualized by BODIPY staining and (c) chlorophyll fluorescence.
(d–f) Mutant 19: (d) bright field, (e) lipids visualized by BODIPY staining, and (f) chlorophyll autofluorescence. Bar: 10 μm.

using starch embedding (Shimogawara *et al.*, 1998). Nonetheless, the high sorting rates mean that the current efficiency of plating recovery is not limiting for the overall throughput.

The CHiLiS approach presented here should be broadly adaptable to other lipid-related screens in *Chlamydomonas*, including screens for mutants that fail to degrade TAG upon re-supply of nitrogen, mutants that have a high lipid content under nitrogen-replete conditions and low-lipid mutants. Importantly, in combination with technologies being developed in our lab for high-throughput, quantitative identification of mutation loci in *C. reinhardtii*, CHiLiS opens the door to genome-wide identification of all genes that are important in lipid metabolism and regulation.

EXPERIMENTAL PROCEDURES

Strains and growth conditions

CMJ030 (deposited in the Chlamydomonas Resource Center as CC-4533) was used as a wild-type background strain. CMJ030 is a cw15 cell-wall-deficient strain that was isolated as a progeny from a cross between $D66^+$ and $4A^-$. Strains 137c and *sta1* were obtained from the Chlamydomonas Resource Center.

For the measurement of lipid accumulation, cells were inoculated from plates to TAP media (Kropat *et al.*, 2011) and grown to 2 million cells ml^{-1} in 25 ml (for individual cultures) or 500 ml (for pooled mutants) volumes shaking at 120 r.p.m. at 25°C under constant light (50 μE m^{-2} sec^{-1}). Lipid accumulation was induced by switching the cells at 2 million cells ml^{-1} to TAP media without nitrogen (TAP-N). Cells were centrifuged at 2000 ***g*** for 5 min, the pellet was resuspended in TAP-N without any NH_4Cl, and the cells were centrifuged again under the same conditions, followed by final resuspension in TAP-N medium (Moellering and Benning, 2010). Cells were kept in TAP-N, shaking at 120 r.p.m. at 25°C under constant light (50 μE m^{-2} sec^{-1}) for 3 days before analysis.

Mutant generation

Mutants were generated as described previously (Zhang *et al.*, 2014).

Cell staining

Cells were spun down (2000 ***g***, 5 min) and resuspended in phosphate-buffered saline (PBS) solution containing 0.011% Triton X-100 to a final cell density of 4 million cells ml^{-1}. For the experiments presented in Figure 3, the indicated concentration of Triton X-100 was used instead. Nile Red was added to the cell culture with a 1:100 dilution from a stock solution of 100 μg ml^{-1} in methanol. The final concentrations during staining were thus 1 μg ml^{-1} Nile Red and 1% methanol. For imaging of mutant 19 (Figure 8a–f), lipids were stained with BODIPY 493/503 (1:100 dilution of 100 μg ml^{-1} in methanol). Cells were vortexed and stained for 15 min in the dark with the tubes being inverted every 3 min for mixing. After staining, cells were spun down again (2000 ***g***, 5 min) and resuspended in PBS.

Cell imaging by microscopy

Confocal imaging of Nile Red-stained cells for emission wavelength information (Figure 2a–d) was performed with a Leica SP5 confocal microscope (http://www.leica.com/). Nile Red-stained cells were immobilized with a 0.5% agarose pad in PBS. Fluorescence was excited at 488 nm, and the emission spectrum was recorded from 508 to 773 nm in 4-nm steps and a bandpass window size of 8 nm. Fluorescence was then excited at 633 nm, and the emission spectrum was recorded from 648 to 786 nm in 3-nm steps and with a bandpass window size of 8 nm.

To image mutant 19 (Figure 8a–f), a Leica DMI6000 inverted microscope was used with a GFP filter cube (excitation filter BP 470/40; dichroic mirror 500; suppression filter BP 525/50) to visualize lipid bodies stained with BODIPY 493/503; a long-pass filter was used to capture lipid droplets and chlorophyll autofluorescence (excitation filter BP 470/40; dichroic mirror 510; suppression filter LP 515).

Flow cytometry and cell sorting

Flow cytometric analyses of single strains were performed on Nile Red-stained cells on a Becton Dickinson (BD) LSR II and cell sorting was performed on a BD FACS Aria II (http://www.bdbiosciences.com/flowcytometry/). For LSRII analysis, Nile Red-stained cells were sampled from a density of 4 million cells ml^{-1} at an analysis rate of about 1000 cells sec^{-1}. For FACS analysis, the cells were concentrated to 10 million cells ml^{-1} at the final PBS resuspension step after staining to enable for a faster sort rate of about 10 000 cells sec^{-1}. Nile Red fluorescence was excited with a 488-nm laser, and emission was captured by a 505-nm longpass splitter with a 525/50 nm bandpass filter. Chlorophyll was excited with a 640-nm laser, and emission was captured by a 670/30-nm bandpass filter.

The distribution of an identically treated culture of CMJ030 was used as a control to set the high lipid gates for mutant sorting. The upper 1% of the wild-type CMJ030 Nile Red/chlorophyll fluorescence signal was set as a high lipid gate. All cells that fell into this gate were collected into vials containing 5 ml TAP media. After sorting, cells were plated onto TAP 2% agar plates in serial dilutions of 250 000, 25 000, 2500 and 250 cells per plate and kept in constant light (10 μE m^{-2} sec^{-1}) for 24 h, and were then transferred to a constant 50 μE m^{-2} sec^{-1} for colony growth.

Lipid extraction and mass spectrometry

For biological replicates, each strain was split into three to six cultures and the cultures underwent at least three back-dilutions in exponential growth in TAP medium, in separate flasks, before the experiment. Cells were grown to mid-log phase [(1–2) $\times$ 10^6 cells ml^{-1}] in TAP and resuspended in TAP-N medium (2 $\times$ 10^6 cells ml^{-1}) as described above. After 3 days under TAP-N conditions, 9 $\times$ 10^6 *C. reinhardtii* cells were spun down (at 3000 ***g*** for 2 min) and total lipids were extracted following the protocol described in Liu *et al.* (2013). Then 13.6 μg of triheptadecanoin (51:0) was added to each sample as an internal standard. This protocol results in total lipids extracted in chloroform. The chloroform was evaporated using a N_2 stream and samples were stored at −80°C. Liquid chromatography–mass spectrometry (LC-MS) and tandem mass spectrometry (MS/MS) analysis were used for neutral lipid profiling of three biological replicates of CMJ030 and each mutant analyzed. The TAG species were characterized by searching the MS and MS/MS fragmentation data against the LipidMaps database (Sud *et al.*, 2007). For analysis, samples were allowed to come to room temperature (20-25°C) and were then resuspended in 1:1 chloroform/methanol and vortexed to mix. For analysis 200 μl was sampled into a clean autosampler vial. The LC-MS analyses were performed with an Agilent 1260 HPLC (http://www.agilent.com/home) and Bruker micrOTOF-Q II mass spectrometer (http://www.bruker.com/) following the methods described by Liu *et al.* (2013). Five microliters of the sample was injected and samples were separated on an Agilent Rapid Resolution Zorbax SB-C18 2.1 $\times$ 30 mm 3.5 μm cartridge column with a flow rate of 0.4 ml min^{-1}. A binary gradient system was used with mobile phase A, consisting of 10 mM ammonium acetate in acetonitrile and water (90:10, v/v), and mobile phase solvent B, with 20 mM ammonium acetate in isopropanol. A linear gradient was used over a 37.5-min run time, with the initial gradient starting at 80% A and 20% B going to 40% A and 60% B. Next, the gradient was increased instantly to 100% B and held for 2.5 min. After this, the system was returned to 80% A and 20% B and held for 5 min. Data were collected in positive electrospray ionization with a full scan mass range of 50–1200 *m*/*z*.

Total fatty acid analysis was conducted on liquid cultures containing 9 $\times$ 10^6 *C. reinhardtii* cells. Twenty micrograms of tridecanoic acid (C13:0 fatty acid) was added as an internal standard, followed by a saponification–transesterification protocol described previously (Work *et al.*, 2010). Pure hexane was used as the extraction reagent. Fatty acid methyl esters (FAME) were analyzed by gas chromatography–flame ionization detection (GC-FID) on a DB-23 column (Agilent) using He as the carrier gas and the following oven profile: hold at 50°C for 1 min; ramp 25°C min^{-1} to 175°C; ramp 4°C min^{-1} to 230°C. Fatty acid methyl esters were quantified against a 37 Component FAME Mix (Supelco, www.supelco.com).

Southern blot

Genomic DNA was extracted from the mutants and their parental strain by phenol–chloroform extraction as described previously (Zhang *et al.*, 2014). Five micrograms was digested overnight with 50 units of *Stu*I. The genomic DNA digests were run at 4°C on a 0.7% TRIS-borate-EDTA (TBE) gel for 17 h at 30 mV, and then for two more hours at 100 mV. The gel was depurinated in 0.25 M HCl for 15 min, and transferred onto a Zeta Probe membrane (Bio-Rad, http://www.bio-rad.com/) in 0.4 M NaOH for 24 h. The blot was rinsed in 2× saline sodium citrate (SSC) buffer and then crosslinked using a UV Stratalinker. Hybridization and signal detection were done following the Amersham Gene Images AlkPhos Direct Labeling and Detection System (GE Healthcare, http://www3.gehealthcare.com/) with the following changes: the primary wash was performed for 3 h and the secondary one for 40 min. The blot was exposed overnight onto CL-XPosure film (Thermo Scientific, http://www.thermoscientific.com/en/home.html) and scanned.

Iodine staining

For the starch staining, cells were transferred either by using a toothpick to pick them directly from stock plates onto TAP-N plates (Figure 4) or by spotting 10^4 cells in 10 μl onto TAP-N plates (Figures 6 and S8). The cells were left on TAP-N plates under constant light (50 μE m^{-2} sec^{-1}) until the colonies became completely yellow (in about 2 weeks). The colonies were stained with iodine vapors to visualize their starch content as previously described (Ball *et al.*, 1991; Zabawinski *et al.*, 2001).

ACKNOWLEDGEMENTS

We thank the Stanford Shared FACS Facility for instrument training, advice and facility services. We thank Xiaobo Li for help with establishing the GC-FID assay and internal TAG controls, and Theresa McLaughlin from the Vincent Coates Foundation Mass Spectrometry Laboratory, Stanford University Mass Spectrometry (http://mass-spec.stanford.edu) for sample measurements and help with analysis. We thank Heather Cartwright, Guido Grossmannn and Lina Duan for training and assistance with the microscopes. We thank Ru Zhang for help with mutant pooling; Spencer Gang and Sean Blum for mutant generation; Xiaobo Li, Mia Jaffe, Ru Zhang, Weronika Patena, Luke Mackinder and Silvia Ramundo for critical reading of the manuscript; and members of the Jonikas lab for helpful discussion. This project was funded by the Carnegie Institution for Science, the US Air Force Office of Scientific Research grant FA9550-11-1-0060 (to M.C.J.), National Institutes of Health training grant T32 GM007276 (to E.S.F.), and US Department of Agriculture National Institute of Food and Agriculture, Agriculture and Food Initiative grant 2011-67012-30652 (to M.T.).

SUPPORTING INFORMATION

Additional Supporting Information may be found in the online version of this article.

Figure S1. Nile Red staining increases the signal in the Nile Red channel but not in the chlorophyll channel.

Figure S2. Nile Red stained cells show bimodal staining when no detergent is added.

Figure S3. The addition of Triton X-100 levels of 0.014% or higher perturbs cellular organization.

Figure S4. Nile Red signal alone, or Nile Red and forward scatter, do not resolve *sta1* from wild-type cells as well as Nile Red and chlorophyll.

Figure S5. The fluorescence-activated cell sorting procedure decreases colony recovery fivefold.

Figure S6. Fatty acid lipidomics reveals increased total fatty acids and altered fatty acid profiles of the mutants.

Figure S7. Southern blot analysis of 10 mutants indicates that each mutant contains one mutagenic cassette insertion.

Figure S8. Original image of 28 isolated mutants spotted on agar and stained with iodine vapors.

Table S1. Normalized median values for Nile Red (NR) and chlorophyll (CHL) fluorescence of mutants measured by flow cytometry, used to generate Figure 6.

Table S2. Lipid species identified using MTQ liquid chromatography–mass spectrometry and tandem mass spectrometry analysis.

Table S3. Fatty acid species identified by gas chromatography–flame ionization detection analyses of the wild type and mutants.

REFERENCES

Ball, S.G., Marianne, T., Dirick, L., Fresnoy, M., Delrue, B. and Decq, A. (1991) A *Chlamydomonas reinhardtii* low-starch mutant is defective for 3-phosphoglycerate activation and orthophosphate inhibition of ADP-glucose pyrophosphorylase. *Planta*, **185**, 17–26.

Boyle, N.R., Page, M.D., Liu, B. *et al.* (2012) Three acyltransferases and nitrogen-responsive regulator are implicated in nitrogen starvation-induced triacylglycerol accumulation in Chlamydomonas. *J. Biol. Chem.* **287**, 15811–15825.

Cagnon, C., Mirabella, B., Nguyen, H.M., Beyly-Adriano, A., Bouvet, S., Cuine, S., Beisson, F., Peltier, G. and Li-Beisson, Y. (2013) Development of a forward genetic screen to isolate oil mutants in the green microalga *Chlamydomonas reinhardtii*. *Biotechnol. Biofuels*, **6**, 178.

Chang, R.L., Ghamsari, L., Manichaikul, A. *et al.* (2011) Metabolic network reconstruction of Chlamydomonas offers insight into light-driven algal metabolism. *Mol. Syst. Biol.* **7**, 518.

Chen, W., Sommerfeld, M. and Hu, Q.A. (2011) Microwave-assisted Nile red method for in vivo quantification of neutral lipids in microalgae. *Bioresour. Technol.* **102**, 135–141.

Chisti, Y. (2008) Biodiesel from microalgae beats bioethanol. *Trends Biotechnol.* **26**, 126–131.

Cirulis, J.T., Strasser, B.C., Scott, J.A. and Ross, G.M. (2012) Optimization of staining conditions for microalgae with three lipophilic dyes to reduce precipitation and fluorescence variability. *Cytometry A*, **81**, 618–626.

Dismukes, G.C., Carrieri, D., Bennette, N., Ananyev, G.M. and Posewitz, M.C. (2008) Aquatic phototrophs: efficient alternatives to land-based crops for biofuels. *Curr. Opin. Biotechnol.* **19**, 235–240.

Doan, T.T.Y. and Obbard, J.P. (2011a) Enhanced lipid production in Nannochloropsis sp. using fluorescence-activated cell sorting. *GCB Bioenergy*, **3**, 264–270.

Doan, T.T.Y. and Obbard, J.P. (2011b) Improved nile red staining of Nannochloropsis sp. *J. Appl. Phycol.* **23**, 895–901.

Doan, T.T.Y. and Obbard, J.P. (2012) Enhanced intracellular lipid in Nannochloropsis sp. via random mutagenesis and flow cytometric cell sorting. *Algal Res.* **1**, 17–21.

Elowitz, M.B., Levine, A.J., Siggia, E.D. and Swain, P.S. (2002) Stochastic gene expression in a single cell. *Science*, **297**, 1183–1186.

Giroud, C., Gerber, A. and Eichenberger, W. (1988) Lipids of *Chlamydomonas reinhardtii*. Analysis of molecular species and intracellular site (s) of biosynthesis. *Plant Cell Physiol.* **29**, 587–595.

Goodson, C., Roth, R., Wang, Z.T. and Goodenough, U. (2011) Structural correlates of cytoplasmic and chloroplast lipid body synthesis in *Chlamydomonas reinhardtii* and stimulation of lipid body production with acetate boost. *Eukaryot. Cell*, **10**, 1592–1606.

Greenspan, P., Mayer, E.P. and Fowler, S.D. (1985) Nile red: a selective fluorescent stain for intracellular lipid droplets. *J. Cell Biol.* **100**, 965–973.

Grobbelaar, J.U. (2010) Microalgal biomass production: challenges and realities. *Photosynth. Res.* **106**, 135–144.

Harris, E.H., Stern, D.B. and Witman, G.B. eds (2009) *The Chlamydomonas Sourcebook*, 2nd edn. San Diego, CA: Academic Press.

Hu, Q., Sommerfeld, M., Jarvis, E., Ghirardi, M., Posewitz, M., Seibert, M. and Darzins, A. (2008) Microalgal triacylglycerols as feedstocks for biofuel production: perspectives and advances. *Plant J.* **54**, 621–639.

Hyka, P., Lickova, S., Pribyl, P., Melzoch, K. and Kovar, K. (2013) Flow cytometry for the development of biotechnological processes with microalgae. *Biotechnol. Adv.* **31**, 2–16.

Kropat, J., Hong-Hermesdorf, A., Casero, D., Ent, P., Castruita, M., Pellegrini, M., Merchant, S.S. and Malasarn, D. (2011) A revised mineral nutrient supplement increases biomass and growth rate in *Chlamydomonas reinhardtii*. *Plant J.* **66**, 770–780.

Li, Y., Han, D., Hu, G., Dauvillee, D., Sommerfeld, M., Ball, S. and Hu, Q. (2010a) Chlamydomonas starchless mutant defective in ADP-glucose pyrophosphorylase hyper-accumulates triacylglycerol. *Metab. Eng.* **12**, 387–391.

Li, Y., Han, D., Hu, G., Sommerfeld, M. and Hu, Q. (2010b) Inhibition of starch synthesis results in overproduction of lipids in *Chlamydomonas reinhardtii*. *Biotechnol. Bioeng.* **107**, 258–268.

Li, X., Benning, C. and Kuo, M.-H. (2012a) Rapid triacylglycerol turnover in *Chlamydomonas reinhardtii* requires a lipase with broad substrate specificity. *Eukaryot. Cell*, **11**, 1451–1462.

Li, X., Moellering, E.R., Liu, B., Johnny, C., Fedewa, M., Sears, B.B., Kuo, M.-H. and Benning, C. (2012b) A galactoglycerolipid lipase is required for triacylglycerol accumulation and survival following nitrogen deprivation in *Chlamydomonas reinhardtii*. *Plant Cell*, **24**, 4670–4686.

Liu, B. and Benning, C. (2012) Lipid metabolism in microalgae distinguishes itself. *Curr. Opin. Biotechnol.* **24**, 300–309.

Liu, X., Clarens, A.F. and Colosi, L.M. (2012) Algae biodiesel has potential despite inconclusive results to date. *Bioresour. Technol.* **104**, 803–806.

Liu, B., Vieler, A., Li, C., Daniel Jones, A. and Benning, C. (2013) Triacylglycerol profiling of microalgae *Chlamydomonas reinhardtii* and *Nannochloropsis oceanica*. *Bioresour. Technol.* **146**, 310–316.

Manandhar-Shrestha, K. and Hildebrand, M. (2013) Development of flow cytometric procedures for the efficient isolation of improved lipid accumulation mutants in a Chlorella sp. microalga. *J. Appl. Phycol.* **25**, 1643–1651.

Merchant, S.S., Kropat, J., Liu, B., Shaw, J. and Warakanont, J. (2012) TAG, you're it! Chlamydomonas as a reference organism for understanding algal triacylglycerol accumulation. *Curr. Opin. Biotechnol.* **23**, 352–363.

Moellering, E.R. and Benning, C. (2010) RNA interference silencing of a major lipid droplet protein affects lipid droplet size in *Chlamydomonas reinhardtii*. *Eukaryot. Cell*, **9**, 97–106.

Montero, M., Aristizabal, M. and Reina, G. (2011) Isolation of high-lipid content strains of the marine microalga *Tetraselmis suecica* for biodiesel production by flow cytometry and sing-cell sorting. *J. Appl. Phycol.* **23**, 1053–1057.

Posewitz, M.C., Smolinski, S.L., Kanakagiri, S., Melis, A., Seibert, M. and Ghirardi, M.L. (2004) Hydrogen photoproduction is attenuated by disruption of an isoamylase gene in *Chlamydomonas reinhardtii*. *Plant Cell*, **16**, 2151–2163.

Riekhof, W.R., Sears, B.B. and Benning, C. (2005) Annotation of genes involved in glycerolipid biosynthesis in *Chlamydomonas reinhardtii*: discovery of the betaine lipid synthase BTA1Cr. *Eukaryot. Cell*, **4**, 242–252.

Shimogawara, K., Fujiwara, S., Grossman, A. and Usuda, H. (1998) High-efficiency transformation of *Chlamydomonas reinhardtii* by electroporation. *Genetics*, **148**, 1821–1828.

Siaut, M., Cuiné, S., Cagnon, C. *et al.* (2011) Oil accumulation in the model green alga *Chlamydomonas reinhardtii*: characterization, variability between common laboratory strains and relationship with starch reserves. *BMC Biotechnol.* **11**, 7.

Stephenson, P.G., Moore, C.M., Terry, M.J., Zubkov, M.V. and Bibby, T.S. (2011) Improving photosynthesis for algal biofuels: toward a green revolution. *Trends Biotechnol.* **29**, 615–623.

Sud, M., Fahy, E., Cotter, D. *et al.* (2007) LMSD: LIPID MAPS structure database. *Nucleic Acids Res.* **35**, D527–D532.

Tonon, T., Harvey, D., Larson, T.R. and Graham, I.A. (2002) Long chain polyunsaturated fatty acid production and partitioning to triacylglycerols in four microalgae. *Phytochemistry*, **61**, 15–24.

Velmurugan, N., Sung, M., Yim, S.S., Park, M.S., Yang, J.W. and Jeong, K.J. (2013) Evaluation of intracellular lipid bodies in *Chlamydomonas reinhardtii* strains by flow cytometry. *Bioresour. Technol.* **138**, 30–37.

Wang, Z.T., Ullrich, N., Joo, S., Waffenschmidt, S. and Goodenough, U. (2009) Algal lipid bodies: stress induction, purification, and biochemical characterization in wild-type and starchless *Chlamydomonas reinhardtii*. *Eukaryot. Cell*, **8**, 1856–1868.

Wijffels, R.H. and Barbosa, M.J. (2010) An outlook on microalgal biofuels. *Science*, **329**, 796–799.

Work, V.H., Radakovits, R., Jinkerson, R.E., Meuser, J.E., Elliott, L.G., Vinyard, D.J., Laurens, L.M., Dismukes, G.C. and Posewitz, M.C. (2010) Increased lipid accumulation in the *Chlamydomonas reinhardtii* sta7-10 starchless isoamylase mutant and increased carbohydrate synthesis in complemented strains. *Eukaryot. Cell*, **9**, 1251–1261.

Xie, B., Stessman, D., Hart, J.H., Dong, H., Wang, Y., Wright, D.A., Nikolau, B.J., Spalding, M.H. and Halverson, L.J. (2014) High-throughput fluorescence-activated cell sorting for lipid hyperaccumulating *Chlamydomonas reinhardtii* mutants. *Plant Biotechnol. J.* **12**, 872–882.

Yan, C., Fan, J. and Xu, C. (2013) Analysis of oil droplets in Microalgae. *Methods Cell Biol.* **116C**, 71–82.

Yao, S., Brandt, A., Egsgaard, H. and Gjermansen, C. (2012) Neutral lipid accumulation at elevated temperature in conditional mutants of two microalgae species. *Plant Physiol. Biochem.* **61C**, 71–79.

Yoon, K., Han, D., Li, Y., Sommerfeld, M. and Hu, Q. (2012) Phospholipid: Diacylglycerol acyltransferase is a multifunctional enzyme involved in membrane lipid turnover and degradation while synthesizing triacylglycerol in the unicellular green Microalga *Chlamydomonas reinhardtii*. *Plant Cell*, **24**, 3708–3724.

Zabawinski, C., Van Den Koornhuyse, N., D'Hulst, C., Schlichting, R., Giersch, C., Delrue, B., Lacroix, J.M., Preiss, J. and Ball, S. (2001) Starchless mutants of *Chlamydomonas reinhardtii* lack the small subunit of a heterotetrameric ADP-glucose pyrophosphorylase. *J. Bacteriol.* **183**, 1069–1077.

Zhang, R., Patena, W., Armbruster, U., Gang, S.S., Blum, S.R. and Jonikas, M.C. (2014) High-throughput genotyping of green algal mutants reveals random distribution of mutagenic insertion sites and endonucleolytic cleavage of transforming DNA. *Plant Cell*, **26**, 1398–1409.